Nonsingular Fast Terminal Sliding Mode Control Approach to Front wheel Subsystem of Steer-by-Wire System

Iman (Eman) Mousavinejad, *Member, IEEE*, Yong Zhu, *Member, IEEE* , Ljubo Vlacic, *Member, IEEE*
Griffith School of Engineering
Griffith University
Australia
eman.mousavinejad@griffithuni.edu.au, y.zhu@griffith.edu.au, l.vlacic@griffith.edu.au

***Abstract*— The steer-by-wire (SbW) system, in which the conventional mechanical linkage between the steering wheel and the front wheel is removed, is capable of acting as an actuator for the active front steering system enhancing vehicle handling performance and safety. Several control strategies have been utilized to control the front wheel subsystem, which is the main part of the SbW system, and the steering response of SbW in the presence of system uncertainties and external disturbance has been improved; however, improvement of the controller transient response is not considered in most of these control strategies. In this paper a nonsingular fast terminal sliding mode (NFTSM) control method for the front wheel subsystem is first established. The NFTSM technique aims to provide a fast transient response for the front wheel tracking controller in the existence of system uncertainties and disturbance including the tire self-aligning torque, Coulomb friction torque and variation of road condition. Simulation results confirm that the proposed nonsingular fast terminal sliding mode controller not only has strong robustness against uncertainties but also improves the transient response of the tracking controller.**

Keywords—steer-by-wire; active front steering; front wheel subsystem; transient response; nonsingular fast terminal sliding mode

NOMENCLATURE

l_f	Distance from front axle to vehicle's center of gravity (CG).
V_x	Vehicle longitudinal speed.
a_y	Vehicle lateral acceleration.
γ	Yaw rate.
β	Vehicle body side slip angle.
C_f	Front, rear tire cornering stiffness.
α_f	Front, rear tire side slip angle.
F_{yf}	Front tire lateral force.
μ	Tire-road friction coefficient.
δ_{wd}	AFS front wheel angle.
δ_w	SbW front wheel angle.
t_p	Tire pneumatic trail.
t_m	Tire mechanical trail.
J_{fw}	Front wheel moment of inertia.
J_{wm}	Front wheel motor moment of inertia.
B_{fw}	Front wheel viscous friction.
B_{wm}	Front wheel motor viscous friction.
N_1, N_2	Rack and pinion gears tooth numbers.
r	Scale factor to account for the conversion from the linear motion of the rack to the rotational motion.
r_g	Actual gear ratio of the front wheel motor and gearhead connection.

I. INTRODUCTION

Steer-by-Wire (SbW) is one of the advanced active steering system actuator technologies in which the steering column between the steering wheel and the front wheel is eliminated and replaced by electronics actuators. The absence of the steering column offers many benefits to vehicle system including more flexibility for locating the steering wheel either in the left or right side of the vehicle and also much more space utilization in the engine compartment, which lead to make the vehicle assembly easier. In addition, the mass of the vehicle is reduced causing increase in vehicle efficiency due to elimination of the steering column and some hydraulics parts.

Undoubtedly the most significant benefits of the steer-by-wire technology are enhancement of the vehicle's safety and handling characteristics. During a frontal crash, there is less probability of steering column intrusion into the driver's survival space. As a result the death toll drastically falls in this type of car accident. Furthermore, with steer-by-wire, the fixed steering system characteristics such as steering effort and steering ratio are adjustable to optimize steering response resulting in the improvement of vehicle handling characteristics.

A lot of research in automotive industry has been conducted on the SbW system and several control strategies have been used to improve steering characteristics.

In [1]-[6], the conventional proportional-derivative (PD) control method was proposed to enable front wheels to follow the driver's steering command. In [7] and [8], a state feedback controller using the linear quadratic regulator (LQR) control technique was introduced to control the rolling angle of the SBW implemented in a motorcycle. In [9], an adaptive controller was designed to control the front wheel actuator through the estimation of the front tire cornering stiffness. In [10], an adaptive online estimation method was used to deal with uncertain parameters of the vehicle motion equipped with the SbW system. In [11], the sliding mode control (SMC) technique was utilized to control the front wheel subsystem of SbW. The front wheel subsystem was modeled using the bond graph method to consider all mechanical and electrical components of this subsystem. The simulation results of the proposed controller demonstrate a good robustness against uncertainties and external disturbance.

It is well known that for both linear and nonlinear systems, the sliding mode control method can be used for tracking controller and stabilization with bounded uncertain parameters of the system [12]. However, SMC does not guarantee that states of the system converge into equilibrium in finite time [13], [14]. In order to deal with the problem of SMC, an advanced type of sliding mode control called nonsingular fast terminal sliding mode (NFTSM) was proposed in [15], which provides a fast and finite convergence time and strong robustness with no singularity problem.

The main contribution of this study is in designing a robust tracking controller and improving the transient response of the front wheel subsystem of SbW in the presence of uncertainties and external disturbance by implementing the nonsingular fast terminal sliding mode method.

The rest of the paper is organized as follows: In section II, the concept of terminal sliding mode control has been reviewed. The procedure for design of the front wheel NFTSM controller has been addressed in section III. Sections IV and V are devoted to simulation results and concluding remarks.

II. Terminal Sliding Mode Control Concept

The terminal sliding mode (TSM) concept is described as [16]

$$s = \dot{x}_1 + \beta' x_1^{q/p} = 0 \tag{1}$$

where $x_1 \in R^1$ is a scalar variable, $\beta' > 0$ and p, q $(p > q)$ are odd positive integers. According to [16], the reaching time to the equilibrium, $x_1 = 0$, is

$$t_s = \frac{p}{\beta'(p-q)} \left| x_1(0) \right|^{\frac{p-q}{p}} \tag{2}$$

If both p and q are considered as $(p = q = 1)$, then the sliding surface defined by (1) can be rewritten as

$$s = \dot{x}_1 + \beta' x_1 = 0 \tag{3}$$

It is obvious that (3) is the definition of sliding surface for the conventional SMC [12]. From (2), the reaching time to the system equilibrium through the sliding surface defined by (3) is $t_s \to \infty$ when $(p = q = 1)$, which means that the system state converges into equilibrium in infinite time, but in TSM, the nonlinear term $x_1^{q/p}$ improves the convergence rate. When the system state is close to equilibrium, the convergence rate is faster resulting in finite reaching time.

However, when the system state is far away from equilibrium, the TSM cannot dominate the linear counterpart since the term $x_1^{q/p}$ tends to reduce the magnitude of the convergence rate at a distance from the equilibrium. To solve this problem, the fast terminal sliding mode (FTSM) surface was expressed as [17]

$$s = \dot{x}_1 + \alpha' x_1 + \beta' x_1^{q/p} = 0 \tag{4}$$

where $\alpha' > 0$. Form (4), it can be concluded that

$$\dot{x}_1 = -\alpha' x_1 - \beta' x_1^{q/p} \tag{5}$$

Equation (5) can be physically interpreted as: when x_1 is far from equilibrium, the approximate dynamic of (5) is expressed as $\dot{x}_1 = -\alpha' x_1$ whose fast convergence can be easily understood [17]. When x_1 is close to equilibrium, the approximate dynamic of (5) becomes $\dot{x}_1 = -\beta' x_1^{q/p}$, which is a terminal attractor. The reaching time to equilibrium is derived as [17]

$$t_s = \frac{p}{\alpha'(p-q)} \ln \frac{\alpha' x_1(0)^{(p-q)/p} + \beta'}{\beta'} \tag{6}$$

Considering the FTSM sliding surface as defined in (4) and a second-order nonlinear system as expressed in (7)

$$\begin{aligned} \dot{x}_1 &= x_2 \\ \dot{x}_2 &= f_1(X) + g_1(X) + b_1(X) u_1 \end{aligned} \tag{7}$$

where $X = [x_1 \quad x_2]^T \in R^2$ are states vector, $u_1 \in R^1$ is the control input, $f_1(X)$ and $b_1(X) \neq 0$ are known nonlinear functions in R^2, $g_1(X)$ is bounded external disturbance and uncertainties, which is $|g_1(X)| \leq k_1'$, the FTSM control law for the system is derived as

$$u_1(t) = -\frac{1}{b_1(X)} \Big(f_1(X) + \alpha' x_2 + \beta' \frac{q}{p} x_1^{(q-p)/p} x_2 + k_1' \operatorname{sgn} s + k_2' s \Big) \tag{8}$$

where k_1', $k_2' > 0$.

The FTSM control law is proven to make the closed-loop control system asymptotically stable in [17]. In (8), the term containing $x_1^{(q-p)/p} x_2$ may cause singularity to occur if

$x_2 \neq 0$ when $x_1 = 0$. This singularity problem may happen in the reaching phase where there is insufficient control to ensure that $x_2 \neq 0$ while $x_1 = 0$. In order to overcome the singularity problem in the FTSM control, the NFTSM surface was proposed in [15] as follows

$$s = x_1 + \alpha' \operatorname{sgn}^{\gamma_1} x_1 + \beta' \operatorname{sgn}^{\gamma_2} x_2 = 0 \tag{9}$$

where $1 < \gamma_2 < 2$, $\gamma_1 > \gamma_2 \in R^1$ and $\operatorname{sgn}^{\gamma_i} x_i = |x_i|^{\gamma_i} \operatorname{sgn} x_i$. To make the system (7) reach the equilibrium fast along the NFTSM sliding surface, the control input is chosen as,

$$u_1 = -\frac{1}{b_1(X)}\left[\frac{1}{\beta'\gamma_2} \operatorname{sgn}^{2-\gamma_2} x_2 \left(1 + \alpha'\gamma_1 |x_1|^{\gamma_1 - 1}\right) + f_1(X) + k_1' \operatorname{sgn} s + k_2' s\right] \tag{10}$$

If the system (7) is controlled by (10), then it is proven that the system is asymptotically stable and reaches to the NFTSM sliding surface (9) in fast-finite time with no singularity during the whole process [15].

III. Front Wheel Controller Design

The front wheel motor controller in the electronic control unit (ECU) controls the front wheel motor torque so that the front wheel subsystem, as shown in Fig. 1, is able to track the commanded front wheel angle by the active front steering system (AFS).

The dynamic equation of the front wheel motor is described by the following second-order differential equation [18]:

$$J_{w,eq}\ddot{\delta}_w + B_{w,eq}\dot{\delta}_w + \tau_f + \tau_a = k_r \tau_m \tag{11}$$

where

$$J_{w,eq} = J_{fw} + \left(\frac{rN_2}{N_1}\right)^2 J_{wm} \tag{12}$$

$$B_{w,eq} = B_{fw} + \left(\frac{rN_2}{N_1}\right)^2 B_{wm} \tag{13}$$

$$k_r = \frac{rN_2}{N_1} r_g \tag{14}$$

where τ_a is the self-aligning torque which reflects the interaction between the road surface and the front wheels while the vehicle is turning, τ_f is the Coulomb friction torque and τ_m is the torque applied on the steering arm by the front wheel motor. The self-aligning and Coulomb friction torques equations are expressed as

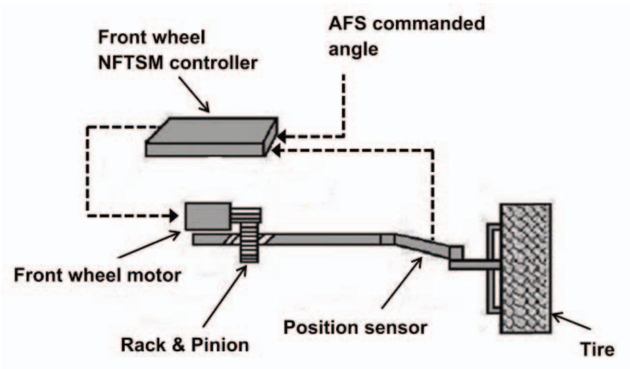

Fig. 1. Front wheel subsystem

$$\tau_a = (t_p + t_m) F_{yf} \tag{15}$$

$$\tau_f = F_f \operatorname{sgn} \dot{\delta}_w \tag{16}$$

where t_p is the pneumatic trail, the distance from the tire center to the application of tire lateral force F_{yf}, t_m is the mechanical trail, the distance between the tire center and the point on the ground about the tire pivots as a result of the wheel caster angle, and F_f is the Coulomb friction constant.

The tire self-aligning and Coulomb friction torques are treated as the most significant uncertainties of the SbW system, which should be bounded as

$$|\tau_a| \leq \bar{\tau}_a \tag{17}$$

$$|\tau_f| \leq \bar{\tau}_f \tag{18}$$

The front-wheel lateral force and sideslip angle can be obtained through the following equations as

$$F_{yf} = -2C_f\, \alpha_f \tag{19}$$

$$\alpha_f = \beta + l_f \frac{\gamma}{V_x} - \delta_w \tag{20}$$

where α_f is the tire slip angle of the front wheel.

Then the upper bound of the self-aligning torque is expressed as

$$\bar{\tau}_a = 2\bar{C}_f\left(\bar{t}_p + \bar{t}_m\right)\left|\left(\beta + \frac{\gamma l_f}{V_x} - \delta_w\right)\right| \tag{21}$$

where $\bar{t}_p$ and $\bar{t}_m$ are the upper bounds of the pneumatic and the mechanical trails, respectively, and $\bar{C}_f$ is the upper bound of the front tire cornering stiffness coefficient.

Remark 1. The front wheel angle, δ_w and the vehicle yaw rate, γ, are measured by using the pinion angle sensor indirectly and the yaw rate sensor respectively. The body sideslip angle, β , can be estimated as

$$\dot{\beta} = \frac{a_y}{V_x} - \gamma \qquad (22)$$

The sideslip angle estimator is not part of this study and can be found in [19].

The upper bound of the Coulomb friction torque is defined as

$$\bar{\tau}_f = \left|\bar{F}_f\right| \mathrm{sgn}\dot{\delta}_w \qquad (23)$$

where $\bar{F}_f$ is the maximum value of the Coulomb friction constant.

According to (7), the states of the system are defined as

$$\begin{aligned} x_1 &= \tilde{\delta}_w \\ x_2 &= \dot{x}_1 = \dot{\tilde{\delta}}_w \end{aligned} \qquad (24)$$

where $\tilde{\delta}_w = \delta_w - \delta_{wd}$, and δ_{wd} is considered as the desired front wheel angle commanded by the active front steering system.

According to (9), the NFTSM surface is chosen as

$$s_w = \tilde{\delta}_w + \alpha'_w \left|\tilde{\delta}_w\right|^{\gamma_{w1}} \mathrm{sgn}\tilde{\delta}_w + \beta'_w \left|\dot{\tilde{\delta}}_w\right|^{\gamma_{w2}} \mathrm{sgn}\dot{\tilde{\delta}}_w \qquad (25)$$

where $1 < \gamma_{w2} < 2$, $\gamma_{w1} > \gamma_{w2} \in R^1$. Considering τ_m, as a control input, from (10) can be calculated that

$$\begin{aligned} \tau_m = -\frac{J_{w,eq}}{k_r}\Bigg(\frac{1}{\beta'_w \gamma_{w2}}\left|\dot{\tilde{\delta}}_w\right|^{2-\gamma_{w2}} \mathrm{sgn}\dot{\tilde{\delta}}_w \big(1 + \\ \alpha'_w \gamma_{w1} \left|\tilde{\delta}_w\right|^{\gamma_{w1}-1}\big) - \frac{B_{w,eq}}{J_{w,eq}}\dot{\tilde{\delta}}_w + \\ k'_{w1} \mathrm{sgn}\, s_w + k'_{w2} s_w\Bigg) \end{aligned} \qquad (26)$$

where k'_{w1}, $k'_{w2} > 0$ and α'_w, $\beta'_w > 0$.

A brushless DC motor can be used to generate the voltage corresponding to the torque calculated by the front wheel motor controller [11].

Proof: According to the NFTSM theorem [15], a positive Lyapunov candidate is considered as

$$V = \frac{1}{2} s_w^2 \qquad (27)$$

The time derivative of the Lyapunov candidate is obtained as

$$\dot{V} = s_w \dot{s}_w \qquad (28)$$

$$\dot{V} = s_w \left(\dot{\tilde{\delta}}_w + \alpha'_w \gamma_{w1} \left|\tilde{\delta}_w\right|^{\gamma_{w1}-1} \dot{\tilde{\delta}}_w + \beta'_w \gamma_{w2} \left|\dot{\tilde{\delta}}_w\right|^{\gamma_{w2}-1} \ddot{\tilde{\delta}}_w \right) \qquad (29)$$

By substituting $\ddot{\tilde{\delta}}_w$ from (11) and τ_m from (26) into (29), then

$$\begin{aligned} \dot{V} = s_w \Bigg(\frac{\beta'_w \gamma_{w2} \left|\dot{\tilde{\delta}}_w\right|^{\gamma_{w2}-1}}{J_{w,eq}} g_w - k'_{w1} \beta'_w \gamma_{w2} \left|\dot{\tilde{\delta}}_w\right|^{\gamma_{w2}-1} \mathrm{sgn}\, s_w \\ - k'_{w2} \beta'_w \gamma_{w2} \left|\dot{\tilde{\delta}}_w\right|^{\gamma_{w2}-1} s_w \Bigg) \end{aligned} \qquad (30)$$

where g_w is an unknown-bounded function of tire self-aligning torque, Coulomb friction torque, and other uncertainties. As $\left|\frac{g_w}{J_{w,eq}}\right| \le k'_{w1}$, it can be concluded that

$$\dot{V} \le -k'_{w2} \beta'_w \gamma_{w2} \left|\dot{\tilde{\delta}}_w\right|^{\gamma_{w2}-1} s_w^2 \qquad (31)$$

$$\dot{V} \le -2k'_{w2} \beta'_w \gamma_{w2} \left|\dot{\tilde{\delta}}_w\right|^{\gamma_{w2}-1} V \quad \rightarrow \dot{V} \le 0 \qquad (32)$$

Therefore, the system can satisfy the Lyapunov stability condition and the system states will reach the NFTSM surface within the fast finite time.

IV. Results and Discussion

To evaluate the performance of the proposed front wheel NFTSM controller, a series of computer simulations are performed with the MATLAB/SIMULINK software. The eight-degree-of-freedom nonlinear vehicle model, which is described and verified in [11], with PACEJKA combined slip tire model [20] are utilized to model the dynamics of the vehicle. Through the simulation process, the active front steering system proposed in [11] is utilized to provide the desired corrective angle for front wheels. The suggested control structure is illustrated in Fig. 2.

According to this control structure, after generating of corrective front wheel angle through the AFS system, the front wheel motor controller produces the required motor torque (26) to generate the AFS-commanded front wheel angle through the SbW system.

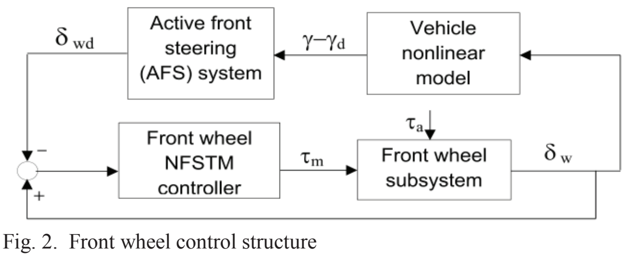

Fig. 2. Front wheel control structure

A. Step Steer Maneuver

One of the critical steering maneuvers is the step steer maneuver, by which the steady state and transient responses of the controller can be evaluated. So, this maneuver is conducted to compare the transient response of the conventional SMC method proposed in [11] and NFTSM strategy to control the front wheel angle. In this maneuver, the vehicle is moving with the speed of 80 km/h on a dry road ($\mu = 0.9$).

As illustrated in Fig. 3, the transient response of SMC has an infinite overshoot and reach steady state response at around 2nd second of simulation time. In addition, the steady state response of SMC is not able to reach the final angle commanded by AFS because of the infinite transient response and chattering occurred in the sliding mode front wheel controller. However, the transient response of the front wheel controller based on NFTSM reaches steady state response in finite time at around 1st second of the simulation time without any overshoot. Moreover, it can be concluded that the NFTSM strategy is able to reduce the chattering phenomenon when the system operates on sliding surface.

Consequently, the NFTSM method enhances the transient response and alleviates the chattering phenomenon of the front wheel controller.

B. Double Lane Change Maneuver

Another typical emergency steering maneuver to evaluate the steering response of a vehicle is the double lane change (DLC) on different road conditions. Therefore, this maneuver is implemented to analyze the performance of the proposed control structure. In this maneuver, the vehicle moves with an initial speed of 105 km/h on a dry road ($\mu = 0.9$) and 80 km/h on a wet road ($\mu = 0.5$).

The front wheel motor torque required for generating the front wheel angle commanded by AFS is demonstrated in Fig. 4. As depicted in Fig. 5, the NFTSM front wheel controller is able to trace the AFS-commanded angle in the presence of the self-aligning and Coulomb friction torques as uncertainties and variation of road condition as external disturbance, which means the front wheel angle can follow

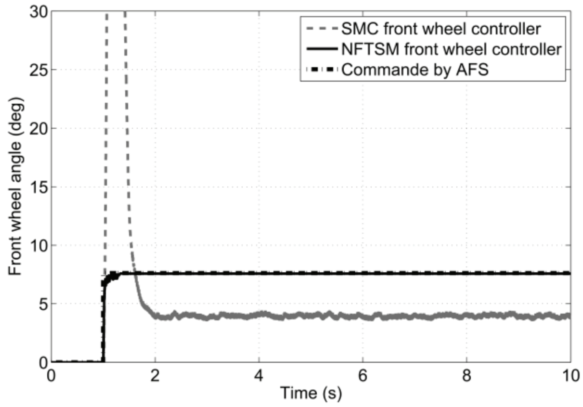

Fig. 3. Comparison between SMC and NFTSM methods

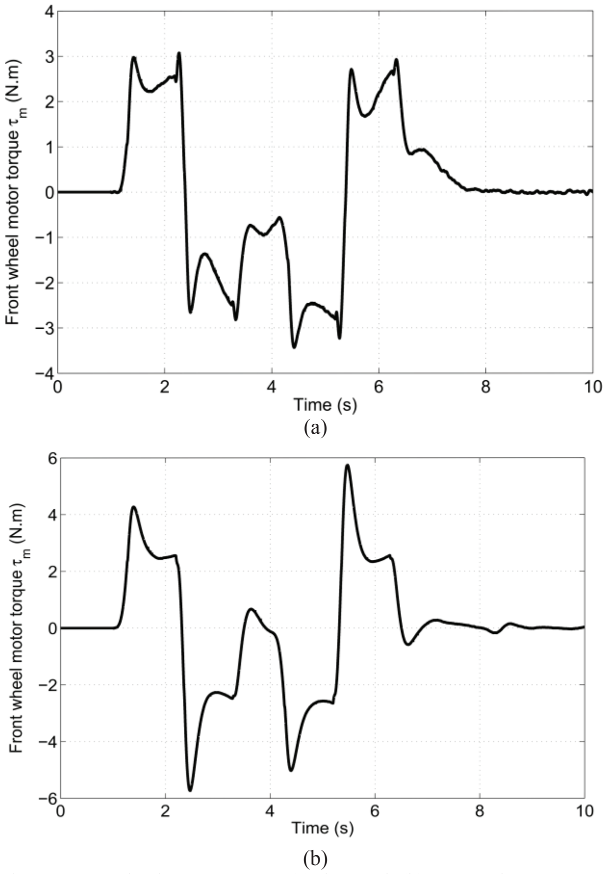

Fig. 4. Front wheel motor torque. (a) dry road. (b) wet road.

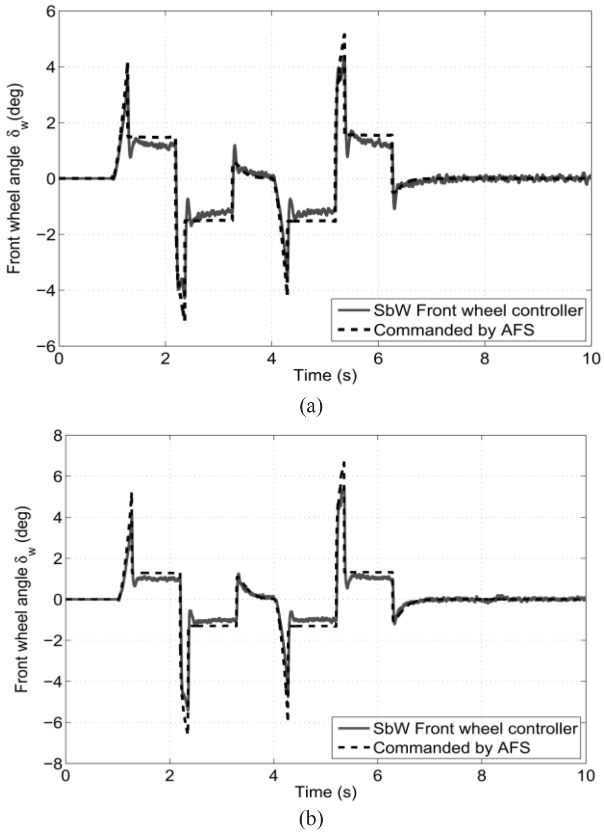

Fig. 5. Front wheel angle. (a) dry road. (b) wet road.

the commanded angle by AFS in fast finite time with strong robustness against uncertain parameters and disturbance.

V. Conclusion and Future Work

The major contribution of this paper is in implementing the nonsingular fast terminal sliding mode control method into the front wheel subsystem of SbW in order to design a robust controller, which can achieve the fast finite transient response in the existence of steering system uncertainties. The simulation outcomes indicate that the NFTSM control strategy improves the transient response of the front wheel tacking controller and also reduces the chattering phenomenon when the system operates in the sliding surface. In addition, the proposed controller demonstrates good robustness against uncertain parameters and disturbance, and excellent tracking performance to follow the front wheel angle commanded by AFS.

Future work of this study will focus on implementation of the advanced type of terminal sliding mode control method to design an integrated vehicle dynamics control structure including steer-by-wire and differential braking systems for ground vehicle, which is under the authors' investigation. Moreover, this study can be further improved through the implementation of the proposed control structure on vehicles for experimental tests in real time.

TABLE I
Vehicle Parameters

Symbol	value
m	1300 kg
l_f	1.2247 m
I_{zz} (unladen)	1808.8 kg m^2
I_{zz} (laden)	1991 kg m^2
C_f	40000N/rad
t_p	0.03 m
t_m	0.02 m
J_{fw}	2.11 kg m^2
J_{wm}	9.8*10^{-4} kg m^2
B_{fw}	12 N/(m/s)
B_{wm}	5.7*10^{-4} N/(m/s)
N_2/N_1	3
r	6.3
r_g	9
F_f	3.2 N.m

TABLE II
Controllers Parameters

Symbol	value
α'_w	20
β'_w	0.005
γ_{w1}, γ_{w2}	1.305, 1.285
k'_{w1}, k'_{w2}	1600, 0.005

References

[1] P. Yih and J. C. Gerdes, "Modification of vehicle handling characteristics via steer-by-wire," *IEEE Trans. Control Syst. Technol.*, vol. 13, no. 6, pp. 965–976, Nov. 2005.

[2] M. Bertoluzzo, G. Buja, and R. Menis, "Control schemes for steer-by-wire systems," *IEEE Ind. Electron. Mag.*, vol. 1, no. 1, pp. 20–27, 2007.

[3] S. W. OH, H. C. Chae, S. C. Yun, and C. S. Han, "The design of a controller for the steer-by-wire system," *JSME Int. J.,* vol. 47, no. 3, pp. 896–907, 2004.

[4] C. J. Kim, J. H. Jang, and S. K. Oh "Development of a control algorithm for a rack-actuating steer-by-wire system using road information feedback," in *Proc. IMechE Part D – J. Automobile Eng.*, vol. 222, no. 9, pp. 1559–1571, Sep.2008.

[5] T. J. Park, C. S. Han, and S. H. Lee, "Development of the electronic control unit for the rack-actuating steer-by-wire using the hardware-in-the-loop simulation system," *Mechatronics*, vol. 15, no. 8, pp. 889–918, Oct. 2005.

[6] P. Setlur, J. R. Wagner, D. M. Dawson, and D. Braganza, "A trajectory tracking steer-by-wire control system for ground vehicles," *IEEE Trans. Veh. Technol.*, vol. 55, no. 1, pp. 76–85, Jan. 2006.

[7] Y. Marumo and M. Nagai, "Steering control of motorcycles using steer-by-wire system," *Veh. Syst. Dyn.*, vol. 45, no. 9, pp. 445–458, May. 2007.

[8] Y. Marumo and N. Katagiri, "Control effects of steer-by-wire system for motorcycles on lane-keeping performance," *Veh. Syst. Dyn.*, vol. 49, no. 8, pp. 1283–1298, Aug. 2011.

[9] Y. Yamaguchi and T. Murakami, "Adaptive control for virtual steering characteristics on electric vehicle using steer-by-wire system," *IEEE Trans. Ind. Electron.*, vol. 56, no. 5, pp. 1585–1594, May 2009.

[10] A. E. Cetin, M. A. Adli, and D. E. Barkana, "Implementation and development of an adaptive steering-control system" *IEEE Trans. Veh. Technol.*, vol. 59, no. 1, pp. 75–83, Jan. 2010

[11] I. Mousavinejad and R. Kazemi, "Variable structure controller design for steer-by-wire system of a passenger car," *J. Mech Sci Technol.*, vol. 28, no. 8, pp. 3285–3299, Aug. 2014.

[12] J. J. E. Slotine and W. Li, *Applied Nonlinear Control,* USA: Prentice Hall, 1991.

[13] I.Mousavinejad, "Advanced terminal sliding mode control approach for integrated steer-by-wire and differential braking of ground vehicles ," Ph.D. dissertation, Engineering Dept., Griffith. Univ., Gold Coast, QLD, unpublished.

[14] I. Mousavinejad, Y. Zhu, and L. Vlacic, "Control strategies for improving vehicle stability, state-of-the-art review," in *Proc. ASCC 2015*, Malaysia, May. 2015.

[15] L. Yang and J. Yang, "Nonsingular fast terminal sliding-mode control for nonlinear dynamical systems," *Int J. Robust Nonlin.*, vol. 21, no. 16, pp. 1865–1879, Nov. 2011.

[16] X. Yu and Z. Man "On finite time mechanism: terminal sliding modes," in *Proc. IEEE-VSS,* Tokyo, 1996, pp. 164–167.

[17] X. Yu and Z. Man, "Fast terminal sliding-mode control design for nonlinear dynamical systems," *IEEE Trans. Circuits Syst. I, Fundom. Theory Appl.*, vol. 49, no. 2, pp. 261–264, Feb. 2002.

[18] Y. H. J. Hsu, S. Laws, and J. C. Gerdes, "Estimation of tire slip angle and friction limits using steering torque," *IEEE Trans. Control. Syst. Technol.*, vol. 18, no. 4, pp. 896–907, Jul. 2010.

[19] M. Abe, A. Kato, K. Suzuki, and Y. Kano, "Estimation of vehicle side-slip angle for DYC by using on-board-tire-model," in *Proc. SAEJ-INT Sym. AVEC*, 1998, pp. 437–442.

[20] H. B. Pacejka, *Tyre and Vehicle Dynamics,* 3rd ed. Butterworth-Heinemann, 2012.